

Four new diarylheptanoids and two new terpenoids from the fruits of *Alpinia oxyphylla* and their anti-inflammatory activities

Jie DONG, Haibo LI, Mi ZHOU, Xinsheng YAO, Jianliang GENG, Yang YU

Citation: Jie DONG, Haibo LI, Mi ZHOU, Xinsheng YAO, Jianliang GENG, Yang YU, Four new diarylheptanoids and two new terpenoids from the fruits of *Alpinia oxyphylla* and their anti-inflammatory activities, *Chinese Journal of Natural Medicines*, 2024, 22(10), 929–936. doi: [10.1016/S1875-5364\(24\)60723-5](https://doi.org/10.1016/S1875-5364(24)60723-5).

View online: [https://doi.org/10.1016/S1875-5364\(24\)60723-5](https://doi.org/10.1016/S1875-5364(24)60723-5)

Related articles that may interest you

[Synthesis, and anti-inflammatory activities of gentiopicroside derivatives](#)

Chinese Journal of Natural Medicines. 2022, 20(4), 309–320 [https://doi.org/10.1016/S1875-5364\(22\)60187-0](https://doi.org/10.1016/S1875-5364(22)60187-0)

[Diversity-oriented synthesis of marine sponge derived hyrtioreticulins and their anti-inflammatory activities](#)

Chinese Journal of Natural Medicines. 2022, 20(1), 74–80 [https://doi.org/10.1016/S1875-5364\(22\)60155-9](https://doi.org/10.1016/S1875-5364(22)60155-9)

[Five new terpenoids from *Viburnum odoratissimum* var. *sessiliflorum*](#)

Chinese Journal of Natural Medicines. 2023, 21(4), 298–307 [https://doi.org/10.1016/S1875-5364\(23\)60438-8](https://doi.org/10.1016/S1875-5364(23)60438-8)

[Anti-inflammatory effects of aucubin in cellular and animal models of rheumatoid arthritis](#)

Chinese Journal of Natural Medicines. 2022, 20(6), 458–472 [https://doi.org/10.1016/S1875-5364\(22\)60182-1](https://doi.org/10.1016/S1875-5364(22)60182-1)

[Anti-inflammatory sesquiterpene polyol esters from the stem and branch of *Tripterygium wilfordii*](#)

Chinese Journal of Natural Medicines. 2023, 21(3), 233–240 [https://doi.org/10.1016/S1875-5364\(23\)60424-8](https://doi.org/10.1016/S1875-5364(23)60424-8)

[Anti-inflammatory effects of *Abelmoschus manihot* \(L.\) Medik. on LPS-induced cystitis in mice: potential candidate for cystitis treatment based on classic use](#)

Chinese Journal of Natural Medicines. 2022, 20(5), 321–331 [https://doi.org/10.1016/S1875-5364\(22\)60140-7](https://doi.org/10.1016/S1875-5364(22)60140-7)



Wechat

•Original article•

Four new diarylheptanoids and two new terpenoids from the fruits of *Alpinia oxyphylla* and their anti-inflammatory activities

DONG Jie^{1Δ}, LI Haibo^{3Δ}, ZHOU Mi¹, YAO Xinsheng^{1*}, GENG Jianliang^{2*}, YU Yang^{1*}

¹ Institute of Traditional Chinese Medicine & Natural Products, College of Pharmacy; International Cooperative Laboratory of Traditional Chinese Medicine Modernization and Innovative Drug Development of Ministry of Education (MOE) of China; and Guangdong Province Key Laboratory of Pharmacodynamic Constituents of TCM and New Drugs Research, Jinan University, Guangzhou 510632, China;

² School of Chinese Materia Medica, Guangdong Pharmaceutical University, Guangzhou 510006, China;

³ State Key Laboratory on Technologies for Chinese Medicine Pharmaceutical Process Control and Intelligent Manufacture, Jiangsu Kanion Pharmaceutical Co., Ltd., Lianyungang 222001, China

Available online 20 Oct., 2024

[ABSTRACT] Four previously unreported diarylheptanoids (**1a/1b–2a/2b**), one undescribed sesquiterpenoid (**8**), one new diterpenoid (**12**), and twelve known analogs were isolated from the fruits of *Alpinia oxyphylla*. The structural elucidation of these compounds was achieved through a comprehensive analysis of spectroscopic data, single-crystal X-ray diffraction, electronic circular dichroism (ECD), and modified Mosher's method. Enantiomeric mixtures (**1a/1b**, **2a/2b**, **3a/3b**, **4a/4b**, and **5a/5b**) were separated on a chiral column using acetonitrile–water mixtures as eluents. Among them, compounds **3a/3b** and **4a/4b** were isolated as optically pure enantiomers in the initial chiral separation. Furthermore, most of the isolates were evaluated for their inhibitory effects against the production of nitric oxide (NO) and interleukin-6 (IL-6) in lipopolysaccharide (LPS)-induced RAW264.7 macrophages. Interestingly, **2** and **4** showed significant inhibitory activities against NO production with IC₅₀ values of 33.65 and 9.88 μmol·L^{−1} (hydrocortisone: IC₅₀ 34.26 μmol·L^{−1}), respectively. Additionally, they also partially reduced the secretion of IL-6.

[KEY WORDS] *Alpinia oxyphylla*; Diarylheptanoids; Terpenoids; Structural elucidation; Anti-inflammatory activity

[CLC Number] R284.1 **[Document code]** A **[Article ID]** 2095-6975(2024)10-0929-08

Introduction

Alpinia oxyphylla (*A. oxyphylla*, Zingiberaceae), known as one of the "four famous south medicines" in China [1], contains a wide range of bioactive compounds, including volatile oil [2], terpenes [3], diarylheptanoids [4] and flavonoids [4]. Among them, diarylheptanoids, composed of two aromatic rings linked by a heptane skeleton, are particularly notable. Modern pharmacological studies have demonstrated that *A. oxyphylla* has multitudinous biological

effects, such as neuroprotective [5, 6], renoprotective [7, 8], anti-inflammatory [9], antioxidant [10], and antitumor [11] activities.

Our recent research identified 40 structurally diverse eudesmane sesquiterpenoids with anti-inflammatory activities, including 17 novel compounds isolated from the fruits of *A. oxyphylla* [12]. In our ongoing investigation to discover additional anti-inflammatory constituents from *A. oxyphylla*, we have isolated and identified two pairs of new diarylheptanoid enantiomers (**1a/1b**, **2a/2b**), one undescribed sesquiterpenoid (**8**), one new diterpenoid (**12**), and twelve known analogs (**3a/3b**, **4a/4b**, **5a/5b**, **6–7**, **9–11** and **13**) (Fig. 1). Except for **6**, all the other compounds were isolated from *A. oxyphylla* for the first time. Among them, compounds **3a/3b** and **4a/4b** were obtained as optically pure enantiomers through chiral separation. The structures of these compounds were elucidated using a combination of comprehensive spectroscopic techniques, including 1D and 2D nuclear magnetic resonance (NMR), infrared spectroscopy (IR), high-resolution electrospray ionization mass spectrometry (HR-ESI-MS), single-crystal X-ray diffraction, electronic circular dichroism

[Received on] 27-Sep.-2023

[Research funding] This work was supported by the Programs Foundation for Leading Talents in National Administration of Traditional Chinese Medicine of China "Qihuang scholars" Project and Basic Research Program Natural Science Fund-Frontier Leading Technology Basic Research Special Project (No. SBK2023050003).

[*Corresponding author] E-mails: tyaoxs@jnu.edu.cn (YAO Xinsheng); gengjianliang8521@126.com (GENG Jianliang); 1018yuyang@163.com (YU Yang)

^ΔThese authors contributed equally to this work.

These authors have no conflict of interest to declare.

(ECD), and the modified Mosher's method. The anti-inflammatory activities of most isolates were evaluated by measuring their inhibitory effects on nitric oxide (NO) and interleukin-6 (IL-6) production in lipopolysaccharide (LPS)-induced RAW264.7 macrophages. Interestingly, **2** and **4** not only showed significant inhibitory activities against NO production with IC_{50} values of 33.65 and $9.88 \mu\text{mol}\cdot\text{L}^{-1}$ (hydrocortisone: IC_{50} $34.26 \mu\text{mol}\cdot\text{L}^{-1}$), but also partially decreased the secretion of IL-6. This study presents the isolation, structural elucidation, and anti-inflammatory activities of these compounds.

Results and Discussion

Structural elucidation of new compounds

Compound **1**, a colorless needle crystal obtained from a methanol-water mixture, was identified as an enantiomeric mixture of **1a** and **1b**. Its HR-ESI-MS spectrum at m/z 329.1758 $[M + H]^+$ (Calcd. for 329.1753) determined a molecular formula of $C_{20}H_{24}O_4$, corresponding to nine degrees of unsaturation. The ^1H NMR spectrum displayed signals characteristic of a monosubstituted benzene ring [δ_{H} 7.28 (2H, m, H-3'', 5''), 7.19 (3H, m, H-2'', 4'', 6''), a 1,2,4-trisubstituted benzene ring [δ_{H} 6.95 (1H, br s, H-2'), 6.88 (2H, d, $J = 7.7$ Hz, H-5', 6')], three oxymethine groups [δ_{H} 4.77 (1H, dd, $J = 11.8, 2.0$ Hz, H-1), 4.35 (1H, m, H-3), 3.96 (1H, m, H-5)], and a methoxyl group [δ_{H} 3.91 (3H, s, 3'-OCH₃)]. The ^{13}C NMR and DEPT spectra resolved 20 carbon resonances: one methoxy (δ_{C} 56.0), four methylenes (δ_{C} 40.6, 38.6, 38.0, 31.8), eleven methines (δ_{C} 128.6×2 , 128.5×2 , 125.8, 118.9,

114.2, 108.9, 73.4, 71.3, 65.2), and four quaternary carbons (δ_{C} 146.5, 144.9, 142.5, 135.2). The above NMR data supported the classification of **1** as a diarylheptanoid. The key heteronuclear multiple bond correlations (HMBCs) of H-1/C-2, 3, 5, 1', 2', 6' and H-7/C-5, 6, 1'', 2'', 6'', together with ^1H - ^1H correlation spectroscopy (COSY) relationships of H-1/H₂-2/H-3/H₂-4/H-5, suggested that the two benzene rings were connected through a pyran ring (Fig. 2). The key nuclear Overhauser effect spectroscopy (NOESY) correlation of H-1/H-5 indicated that H-1 and H-5 were on the same face of the molecule (Fig. 2). Subsequently, **1** was separated into a pair of enantiomers **1a** and **1b** via chiral separation (Fig. S10). The absolute configurations of **1a** and **1b** were further confirmed as 1*S*,3*S*,5*S* and 1*R*,3*R*,5*R*, respectively, by single-crystal X-ray diffraction using Cu K α radiation (Fig. 3). Consequently, compounds **1a** and **1b** were finally identified as (1*S*,3*S*,5*S*)-3-hydroxy-1,5-epoxy-1-(4-hydroxy-3-methoxyphenyl)-7-phenyl-3-heptanol and (1*R*,3*R*,5*R*)-3-hydroxy-1,5-epoxy-1-(4-hydroxy-3-methoxyphenyl)-7-phenyl-3-heptanol, respectively.

Compound **2**, a yellow oil, was obtained as a mixture of enantiomers (**2a** and **2b**). It showed a $[M + H]^+$ ion peak at m/z 357.2067 (Calcd. for 357.2066), consistent with the molecular formula of $C_{22}H_{28}O_4$. A comparison of the spectral data of **2** and **4** [13] revealed that a hydroxy group in **4** was replaced by an acetoxy group in **2**, which was confirmed by HMBCs of H-3/C-8 and H₃-9/C-8. Additionally, the absence of a hydroxyl group at C-4 in **2** was indicated by the high-field chemical shifts for C-4 (δ_{C} 34.1/ δ_{H} 1.60). Further, **2** was

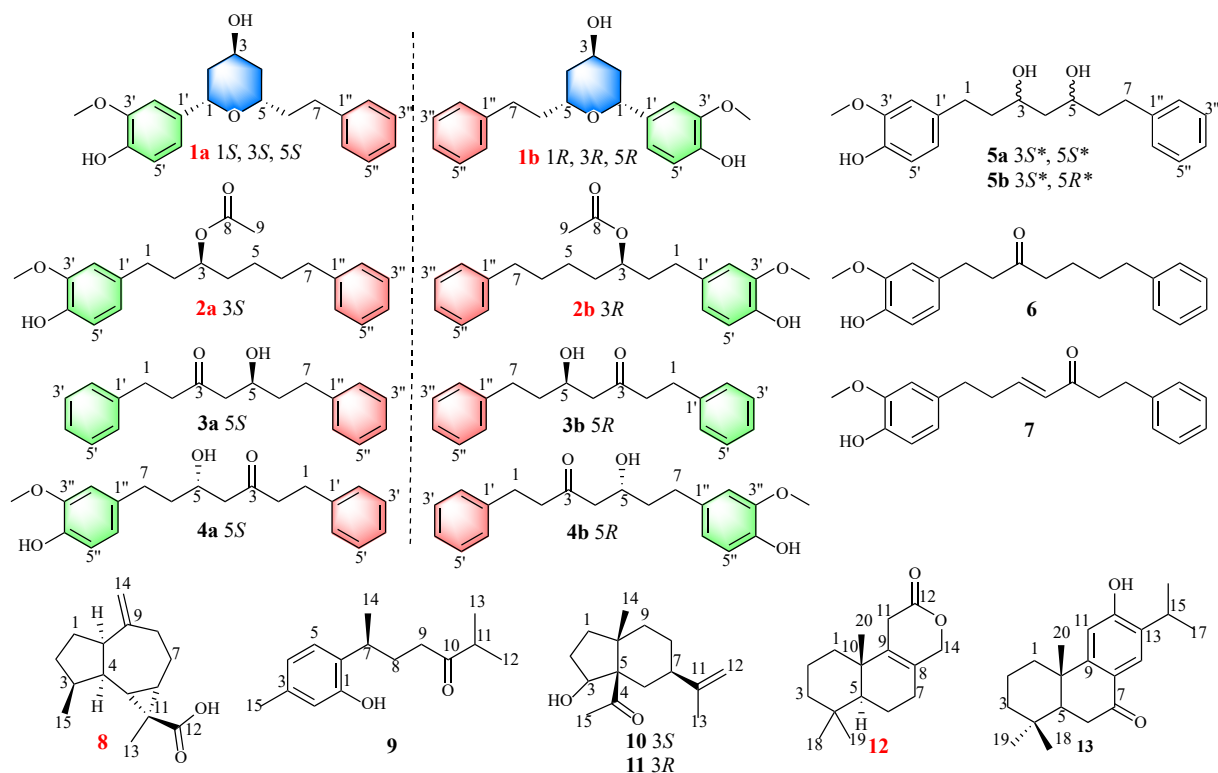


Fig. 1 Chemical structures of compounds **1a**–**13** (red: new compounds).

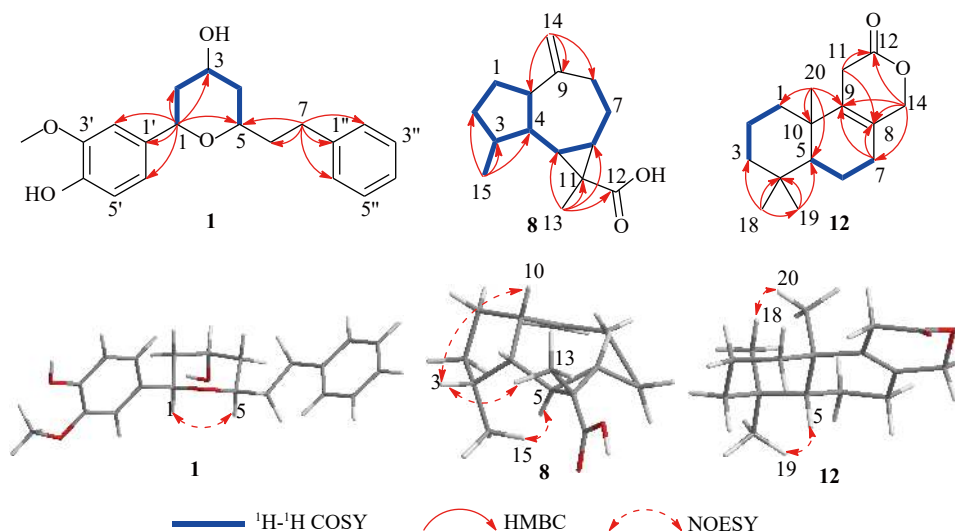


Fig. 2 Key ^1H - ^1H COSY, HMBC, and NOESY correlations of compounds **1**, **8**, and **12**.

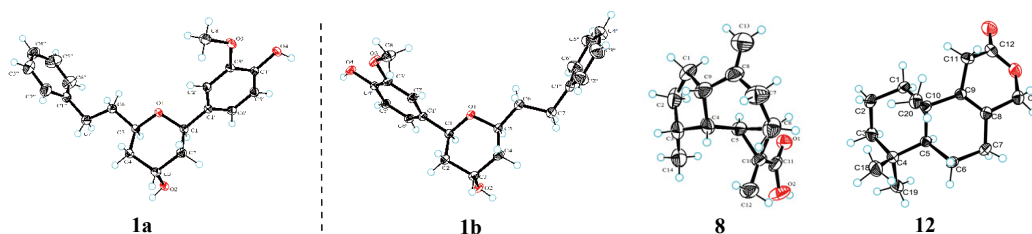


Fig. 3 X-ray ORTEP diagrams of compounds **1a**, **1b**, **8**, and **12**.

separated into a pair of enantiomers **2a** and **2b** via chiral separation (Fig. S20). The absolute configuration at C-3 was determined using acid hydrolysis and the modified Mosher's method. Based on differences in ^1H NMR data (Figs. S21 and S22), the structures of **2a** and **2b** were determined (Fig. 1) as (3*S*)-3-acetoxy-1-(4-hydroxy-3-methoxyphenyl)-7-phenylheptane and (3*R*)-3-acetoxy-1-(4-hydroxy-3-methoxyphenyl)-7-phenylheptane, respectively.

Compound **8**, obtained as a colorless needle crystal (methanol-acetone), was determined to have molecular formula $\text{C}_{15}\text{H}_{22}\text{O}_2$ based on its ^{13}C NMR and HR-ESI-MS data at m/z 235.1688 $[\text{M} + \text{H}]^+$ (Calcd. for 235.1698). Comparison of the NMR data of **8** and that of (4*R*,5*S*,6*R*,7*R*,11*S*)-2-oxo-1(10)-aromadendren-12-oic^[14] revealed a similar core structure, with the key difference being the absence of a carbonyl group at C-1 and the position of the double bond. The chemical shifts for C-1 (δ_{H} 1.92, 1.77; δ_{C} 28.2) suggested that the carbonyl group was reduced to a methylene group in **8**. Moreover, the HMBCs from H_2 -14 (δ_{H} 4.79, 4.76) to C-8, C-9, and C-10 confirmed the presence of a double bond at C6 (7) in **8**. The NOESY correlations of H-3/H-10, H_3 -13 and H-5/ H_3 -15 suggested that H-3, H-10, and H_3 -13 were oriented in the same direction, while H-5 and H_3 -15 were oriented in the opposite orientation (Fig. 2). The relative configuration of **8** was further confirmed as 3*R**,4*R**,5*R**,6*S**,10*S**,11*S** by single-crystal X-ray diffraction using Cu K α radiation

(Fig. 3). While the absolute configurations of **8** was finally determined to be 3*S*,4*S*,5*S*,6*R*,10*R*,11*R* by comparison of their experimental and calculated ECD spectra (Fig. 4). Consequently, **8** was finally identified as aromodendrone A.

Compound **12** was isolated as a colorless crystal (methanol-water). Its HR-ESI-MS spectrum at m/z 249.1856 $[\text{M} + \text{H}]^+$ (Calcd. for 249.1855) confirmed its molecular formula as $\text{C}_{16}\text{H}_{24}\text{O}_2$. The ^1H and ^{13}C data of **12** were highly similar to those of 2*H*-naphtho[2,1-*c*]pyran-7-carboxylic acid^[15], with the key difference being a methyl group at C-4 instead of a carbomethoxy group, as confirmed by the NMR data. The relative configuration of **12** was inferred by the NOESY correlations of H_3 -18/ H_3 -20 and H_3 -19/H-5. Finally, the absolute

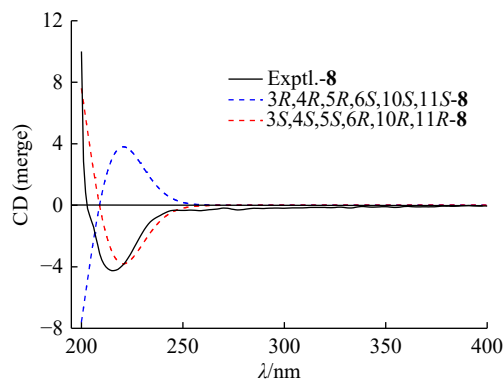


Fig. 4 Experimental and calculated ECD spectra of **8**.

configuration of **12** was established to be 5*S*, 10*S* by single-crystal X-ray diffraction experiment with Cu K α radiation (Fig. 3). Therefore, based on the above evidence, **12** was identified as oxyditerone A.

The remaining 12 known compounds were identified by comparison with the previously reported data in the literature: (5*S*)-/(5*R*)-dihydroxyashabushiketol (**3a/3b**)^[16], (5*S*)-/(5*R*)-5-hydroxy-7-(4-hydroxy-3-methoxyphenyl)-1-phenyl-3-heptanone (**4a/4b**)^[17], (3*S**,5*S**)-/(3*S**,5*R**)-1-(4-hydroxy-3-methoxyphenyl)-7-phenyl-3,5-heptanediol (**5a/5b**)^[13], yakuchinone A (**6**)^[18], (4*E*)-7-(4-hydroxy-3-methoxyphenyl)-1-phenyl-4-hepten-3-one (**7**)^[18], 1-hydroxy-1,3,5-bisabolatrien-10-one (**9**)^[19], cyperolone (**10**)^[20], 3-*epi*-cyperolone (**11**)^[20], and sugiol (**13**)^[21].

Anti-inflammatory effects of isolates in LPS-stimulated RAW264.7 cells

Compounds **2–4**, **6**, and **12** were evaluated for their inhibitory effects against the production of NO in LPS-induced RAW264.7 macrophages. Due to the limited quantities of enantiomers (**2–4**) after chiral separation, we conducted an activity evaluation on the enantiomeric mixtures. As a result, **2** and **4** showed significant inhibitory activities against NO production in LPS-stimulated RAW 264.7 macrophages, with IC₅₀ values of 33.65 and 9.88 $\mu\text{mol}\cdot\text{L}^{-1}$ (hydrocortisone: IC₅₀ 34.26 $\mu\text{mol}\cdot\text{L}^{-1}$), respectively (Fig. 5). Additionally, **2** and **4** could partially decrease the secretion of IL-6 in a dose-dependent manner (Fig. 6). No obvious cytotoxicity of these compounds at the testing concentrations was detected by the 3-(4,5-dimethylthiazol-2-yl)-2,5-diphenyl-2H-tetrazolium bromide (MTT) assay (Fig. S47).

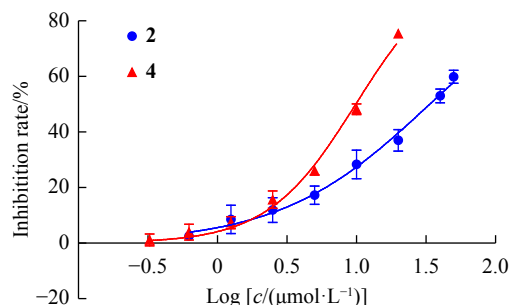


Fig. 5 Inhibitory effects of compounds on LPS-induced NO generation in RAW264.7 cells (mean \pm SD, $n = 3$).

Experimental

General experimental procedures

Optical rotations were measured at room temperature using a JASCO P1020 polarimeter (JASCO, Japan). UV spectra were recorded with a JASCO V550 (JASCO, Japan) instrument, and IR spectra were acquired using a JASCO FT/IR-480 plus spectrometer (KBr) (JASCO, Japan). NMR spectra were obtained on Bruker AV-400/600 MHz NMR spectrometers (Bruker, Switzerland) with solvent signals (CDCl_3 : δ_{H} 7.26/ δ_{C} 77.2; $\text{C}_5\text{D}_5\text{N}$: δ_{H} 7.58/ δ_{C} 135.9,) as an internal reference. HR-ESI-MS spectra were recorded on a Waters Synapt

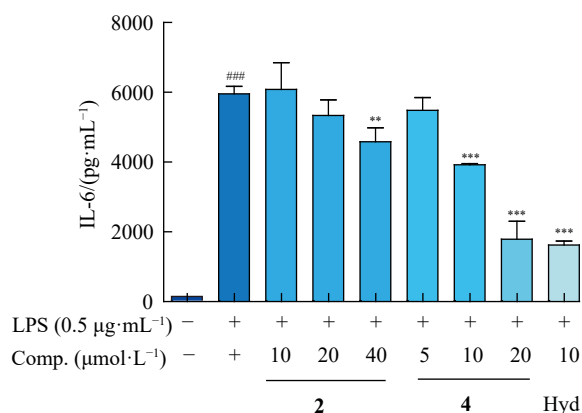


Fig. 6 IL-6 secretion in the supernatant of RAW264.7 cells of controls, LPS, and compounds treated under LPS (mean \pm SD, $n = 3$). ### $P < 0.001$ vs Control, * $P < 0.05$, ** $P < 0.01$, *** $P < 0.001$ vs LPS. Hyd: hydrocortisone

G2 mass spectrometer (Waters, USA). Analytical HPLC (SHIMADZU, Japan) was conducted on a Shimadzu HPLC system with an LC-20AB solvent delivery system and an SPD-20A UV/vis detector using a Phenomenex Gemini C₁₈ column (5 μm , 4.6 mm \times 250 mm, Phenomenex Gemini, USA). Semipreparative HPLC (SHIMADZU, Japan) was conducted on a Shimadzu LC-6AD liquid chromatography system equipped with an SPD-20A detector on a Phenomenex Gemini C₁₈ column (5 μm , 10.0 mm \times 250 mm) and preparative HPLC using a Phenomenex Gemini C₁₈ column (5 μm , 20.0 mm \times 250 mm). Diaion HP-20 (Mitsubishi Chemical Co., Japan), silica gel (100–200 and 200–300 mesh, Qingdao Marine Chemical Co., China), MCI gel CHP20P (75–150 μm , Mitsubishi Chemical Co., Japan), Sephadex LH-20 (GE Healthcare, Britain), and octadecyl silane (ODS) silica gel (12 nm, S-50 μm , YMC, Britain) were used for column chromatography (CC). Thin-layer chromatography (TLC) was performed using precoated silica gel GF₂₅₄ plates (Qingdao Marine Chemical Co., China). HPLC-grade methanol and acetonitrile (China) were bought from Macklin Biochemical Co., Ltd., and all analytical-grade reagents were obtained from Concord Chemicals Co., Ltd. (China).

Plant material

The dried fruits of *A. oxyphylla* were purchased from Anguo Shiyuan Trading Co., Ltd. in September 2020, which were authenticated by Prof. ZHOU Guangxiong (Jinan University). A voucher specimen (No. JNU2020AO101) was deposited at the Institute of Traditional Chinese Medicine & Natural Products, College of Pharmacy, Jinan University, Guangzhou, China.

Extraction and isolation

The broken fruits (60.0 kg) of *A. oxyphylla* were extracted twice with 60% EtOH (360 L) by refluxing for 2 h each time. The combined extracts (AOEs, 9.8 kg) were obtained by evaporation under reduced pressure. These AOEs were then fractionated using HP-20 resin CC, eluted with an ethanol-water gradient, yielding four fractions (Frs. AO-1–AO-4). Fr. AO-3 (292 g) and Fr. AO-4 (325 g) were further separ-

ated using silica gel CC (200–300 mesh, $\Phi 12\text{ cm} \times 75\text{ cm}$) eluting with a cyclohexane–EtOAc (99 : 1 to 0 : 1, *V/V*) gradient, yielding 10 sub-fractions (Frs. AO3A–AO3J) and 13 sub-fractions (Frs. AO4A–AO4M), respectively.

Fr. 3F (53.9 g) was subjected to ODS CC (MeOH/H₂O), resulting in Frs. 3F1–3F5. Fr. 3F5 (4.1 g) was purified by semipreparative HPLC using ACN/H₂O (35 : 65, *V/V*) as the mobile phase, yielding compounds **4** (6.6 mg, *t_R* 15.5 min), **5** (3.2 mg, *t_R* 16.6 min), and **1** (6.3 mg, *t_R* 18.4 min), respectively.

Fr. 4E (46.3 g) was separated by ODS CC (MeOH/H₂O), resulting in Frs. 4E1–4E11. Fr. 4E6 (30.7 g) further fractionated using silica gel CC (200–300 mesh, $\Phi 2.6\text{ cm} \times 60\text{ cm}$) eluting with a cyclohexane–EtOAc (100 : 0 to 0 : 1, *V/V*) gradient, yielding 12 sub-fractions (Frs. E6A–E6L). Fr. E6G (1.9 g) and Fr. E6H (1.4 g) were purified by semipreparative HPLC to obtain compounds **8** (4.4 mg, *t_R* 12.5 min, 70% MeOH), **12** (1.2 mg, *t_R* 18.0 min, 60% ACN), **9** (3.2 mg, *t_R* 15.5 min, 60% ACN), and **13** (1.2 mg, *t_R* 17.0 min, 60% ACN), respectively. Fr. 4G (10.7 g) was separated by ODS CC (MeOH/H₂O), resulting in Frs. 4G1–4G8. Frs. 4G5 (2.5 g), Fr. 4G7 (3.7 g), and 4G8 (530.1 mg) were purified by semipreparative HPLC to isolate compounds **3** (9.1 mg, *t_R* 30.0 min, 50% ACN), **10** (11.1 mg, *t_R* 25.0 min, 50% ACN) and **11** (6.0 mg, *t_R* 26.0 min, 50% ACN), **7** (6.5 mg, *t_R* 20.0 min, 50% ACN), **6** (22.1 mg, *t_R* 21.0 min, 40% ACN), and **2** (6.2 mg, *t_R* 17.5 min, 75% MeOH), respectively.

Compound **1** was further separated by semipreparative chiral HPLC (EnantioPak Y3, 5 μm , 250 mm \times 4.60 mm, 40% ACN, 1 mL·min^{−1}), yielding **1a** (2.3 mg, *t_R* 14.0 min) and **1b** (2.0 mg, *t_R* 16.0 min). Compound **2** was further separated by semipreparative chiral HPLC (EnantioPak AY, 5 μm , 250 mm \times 4.60 mm, 60% ACN, 1 mL·min^{−1}), yielding **2a** (1.3 mg, *t_R* 8.0 min) and **2b** (1.8 mg, *t_R* 9.0 min). Compounds **3–5** were further separated by semipreparative chiral HPLC (EnantioPak Y1, 5 μm , 250 mm \times 4.60 mm, 85% ACN, 1 mL·min^{−1}), yielding **3a** (0.6 mg, *t_R* 9.5 min), **3b** (0.7 mg, *t_R* 20.0 min), **4a** (0.9 mg, *t_R* 6.5 min), **4b** (1.4 mg, *t_R* 16.0 min), **5a** (0.6 mg, *t_R* 17.6 min), and **5b** (0.9 mg, *t_R* 20.2 min).

Identification of new compounds

(1*S*,3*S*,5*S*)/(1*R*,3*R*,5*R*)-3-hydroxy-1,5-epoxy-1-(4-hydroxy-3-methoxyphenyl)-7-phenyl-3-heptanol (**1a/1b**): Colorless crystal (methanol–water); $[\alpha]_{\text{D}}^{27}$ −4.4 (*c* 0.5, CHCl₃, **1a**), $[\alpha]_{\text{D}}^{27}$ +4.4 (*c* 0.5, CHCl₃, **1b**); HR-ESI-MS (positive) *m/z* 329.1758 [*M* + *H*]⁺ (Calcd. for C₂₀H₂₅O₄, 329.1753); UV (MeOH) λ_{max} (log ϵ): 202 (4.84) nm; IR (KBr) ν_{max} : 3550.96, 3415.90, 3238.37, 2937.23, 2925.35, 2859.25, 1637.26, 1617.80, 1527.78, 1453.93, 1385.38, 1269.11, 1158.74, 1133.46, 1055.88, 963.32, 853.28, 702.05, 618.15, 474.87 cm^{−1}; NMR data (Table 1).

Crystal data for 1a: [(1*S*,3*S*,5*S*)-3-hydroxy-1,5-epoxy-1-(4-hydroxy-3-methoxyphenyl)-7-phenyl-3-heptanol] C₂₀H₂₄O₄ (*Mr*: 328.39): monoclinic, space group P2₁ (no. 4), *a* = 8.85787 (19) Å, *b* = 5.55758 (14) Å, *c* = 17.7214 (4) Å, β = 93.5084 (19)°, *V* = 870.76 (3) Å³, *Z* = 2, *T* = 149.99 (10)

K, $\mu(\text{Cu K}\alpha)$ = 0.696 mm^{−1}, *D*_{calc} = 1.252 g/cm³, 9010 reflections measured (4.996° ≤ 2 θ ≤ 147.646°), and 3332 unique (*R*_{int} = 0.0368, *R*_{sigma} = 0.0355) which were used in all calculations. Final *R*₁ = 0.0319 (*I* > 2 σ (*I*)), final *wR*₂ = 0.0863 (all data), Flack = 0.10 (10), and CCDC number: 2256762.

Crystal data for 1b: [(1*R*,3*R*,5*R*)-3-hydroxy-1,5-epoxy-1-(4-hydroxy-3-methoxyphenyl)-7-phenyl-3-heptanol] C₂₀H₂₄O₄ (*Mr*: 328.39): monoclinic, space group P2₁ (no. 4), *a* = 8.85860 (10) Å, *b* = 5.55890 (10) Å, *c* = 17.7216 (4) Å, β = 93.522 (2)°, *V* = 871.04 (3) Å³, *Z* = 2, *T* = 150.00 (10) K, $\mu(\text{Cu K}\alpha)$ = 0.696 mm^{−1}, *D*_{calc} = 1.252 g/cm³, 15974 reflections measured (4.996° ≤ 2 θ ≤ 147.892°), 3358 unique (*R*_{int} = 0.0840, *R*_{sigma} = 0.0550) which were used in all calculations. Final *R*₁ = 0.0508 (*I* > 2 σ (*I*)), final *wR*₂ = 0.1293 (all data), Flack = 0.07(18), and CCDC number: 2257164.

(3*S*)/(3*R*)-3-acetoxy-1-(4-hydroxy-3-methoxyphenyl)-7-phenylheptane (**2a/2b**): yellow oil; $[\alpha]_{\text{D}}^{27}$ −2.0 (*c* 0.5, CHCl₃, **2a**), $[\alpha]_{\text{D}}^{27}$ +2.0 (*c* 0.5, CHCl₃, **2b**); HR-ESI-MS (positive) *m/z* 357.2067 [*M* + *H*]⁺ (Calcd. for C₂₂H₂₉O₄, 357.2066); UV (MeOH) λ_{max} (log ϵ): 203 (4.45), 282 (3.28) nm; IR (KBr) ν_{max} : 3449, 3026, 2935, 1732, 1637, 1516, 1454, 1431, 1384, 1243, 1153, 1122, 1033, 797, 748, 700, 473 cm^{−1}; NMR data (Table 1).

Aromodendrone A (**8**): Colorless crystal (methanol–acetone). $[\alpha]_{\text{D}}^{27}$ −9.6 (*c* 0.5, CHCl₃). HR-ESI-MS (positive) *m/z* 235.1688 [*M* + *H*]⁺ (Calcd. for C₁₅H₂₃O₂, 235.1698); UV (MeOH) λ_{max} (log ϵ): 202 (4.50); IR (KBr) ν_{max} : 3448, 2956, 2870, 1670, 1633, 1468, 1421, 1394, 1298, 1261, 1099, 1041, 884, 615, 547 cm^{−1}; NMR data (Table 1).

Crystal data for 8: C₁₅H₂₂O₂ (*Mr*: 234.32): orthorhombic, space group P2₁2₁2₁ (no. 19), *a* = 6.0840(8) Å, *b* = 15.424(4) Å, *c* = 28.249(5) Å, *V* = 2650.8(9) Å³, *Z* = 4, *T* = 169.99(10) K, $\mu(\text{Cu K}\alpha)$ = 0.297 mm^{−1}, *D*_{calc} = 0.587 g/cm³, 6744 reflections measured (6.258° ≤ 2 θ ≤ 147.166°), 4657 unique (*R*_{int} = 0.0896, *R*_{sigma} = 0.1687) which were used in all calculations. Final *R*₁ was 0.0913 (*I* > 2 σ (*I*)), final *wR*₂ = 0.2473 (all data), and Flack = −0.40(7).

Oxyditerone A (**12**): Colorless crystal (methanol–water). $[\alpha]_{\text{D}}^{27}$ +200 (*c* 0.5, CHCl₃). HR-ESI-MS (positive) *m/z* 249.1856 [*M* + *H*]⁺ (Calcd. for C₁₆H₂₅O₂, 249.1855); UV (MeOH) λ_{max} (log ϵ): 204 (4.40) nm; IR (KBr) ν_{max} : 2998, 2926, 1746, 1685, 1654, 1630, 1458, 1401, 1231, 1154, 1040 cm^{−1}; NMR data (Table 1).

Crystal data for 12: C₁₅H₂₄O₂ (*Mr*: 236.34): orthorhombic, space group P2₁2₁2₁ (no. 19), *a* = 6.07490(10) Å, *b* = 7.88170(10) Å, *c* = 28.1968(6) Å, *V* = 1350.08(4) Å³, *Z* = 4, *T* = 293(2) K, $\mu(\text{Cu K}\alpha)$ = 0.584 mm^{−1}, *D*_{calc} = 1.163 g/cm³, 7757 reflections measured (6.268° ≤ 2 θ ≤ 147.432°), 2686 unique (*R*_{int} = 0.0230, *R*_{sigma} = 0.0237) which were used in all calculations. Final *R*₁ was 0.0304 (*I* > 2 σ (*I*)), final *wR*₂ = 0.0794 (all data), and Flack = −0.06(9).

Modified Mosher's reaction

To a solution of **2b** (1.8 mg) in MeOH (1.0 mL), a drop of analytical-grade HCl was added. The resulting mixture was stirred at room temperature overnight and then dried un-

Table 1 ^1H and ^{13}C NMR data of compounds **1**, **2**, **8** and **12** in CDCl_3 (600 MHz)

No.	1		2		8		12	
	δ_{C}	δ_{H} (J in Hz)	δ_{C}	δ_{H} (J in Hz)	δ_{C}	δ_{H} (J in Hz)	δ_{C}	δ_{H} (J in Hz)
1	73.4	4.77, dd (11.8, 2.0)	31.6	2.52	28.2	1.92 1.77	35.9	1.68 1.08, td (12.7, 3.8)
2	40.6	1.93 1.77	36.3	1.82	31.2	1.77 1.38	18.8	1.61 1.53
3	65.2	4.35	73.9	4.92	37.8	2.12	41.7	1.45 1.17
4	38.6	1.93 1.77	34.1	1.60	41.5	1.92	33.4	
5	71.3	3.96	25.0	1.34	27.8	1.33	51.5	1.19
6	38.0	1.71 1.64	31.4	1.60	28.0	1.60	18.3	1.79 1.49
7	31.8	2.83 2.73	35.9	2.60, t (7.8)	22.1	1.92 1.33	27.2	2.00
8			171.1		34.6	2.37 2.26	123.0	
9			21.4	2.04, s	151.2		134.9	
10					50.7	2.71	37.1	
11					25.2		28.9	2.97
12					182.8		171.4	
13					9.8	1.22, s		
14					111.0	4.79, br s 4.76	71.5	4.64 4.57
15					16.3	0.94, d (6.9)		
18							21.6	0.86, s
19							33.3	0.91, s
20							19.5	1.00, s
1'	135.2		133.7					
2'	108.9	6.95	111.1	6.65				
3'	146.5		146.5					
4'	144.9		143.9					
5'	114.2	6.88	114.4	6.83, d (7.7)				
6'	118.9	6.88	120.9	6.65				
1''	142.5		142.6					
2''	128.5	7.19	128.4	7.17				
3''	128.6	7.28	128.5	7.27				
4''	125.8	7.19	125.8	7.17				
5''	128.6	7.28	128.5	7.27				
6''	128.5	7.19	128.4	7.17				
3'-OCH ₃	56.0	3.91, s	56.0	3.87, s				
4'-OH		5.47, s						

Multiplets and or overlapped signals are reported without designating multiplicity.

der vacuum. Compounds **2b** and **4a** (0.4 mg) were each divided equally into two NMR tubes and dried under vacuum for 12 h. To each NMR tube containing compounds **2b** and **4a** (0.4 mg), anhydrous pyridine (400 μL) was added, followed by the addition of (*R*)-MTPA (10 μL) and (*S*)-MTPA (10 μL), respectively. The reaction was performed at 4 $^{\circ}\text{C}$ and monitored by 600 MHz NMR.

ECD calculations for compound **8**

The ECD spectra of compound **8** were calculated using Gaussian 09 software. Firstly, a conformational search was conducted using the MMFF force field in Discovery Studio 3.5 Client, with an energy threshold of 17 $\text{kJ}\cdot\text{mol}^{-1}$ (approximately 4 $\text{kcal}\cdot\text{mol}^{-1}$). Next, all identified conformations were optimized at the B3LYP/6-31G(d) level of theory. Following optimization, the ECD spectra of the conformations were calculated at the B3LYP/6-311 + G(d,p) level of theory. Finally, the individual ECD spectra were combined and weighted according to their Boltzmann distribution based on the relative energies of the conformations.

Anti-inflammatory activities assays

Cell culture. RAW264.7 macrophages were obtained from the American Type Culture Collection (ATCC) and cultured in Dulbecco's Modified Eagle Medium (DMEM, Thermo Fisher Scientific) supplemented with 10% fetal bovine serum (FBS, Excell Bio), 100 $\text{U}\cdot\text{mL}^{-1}$ penicillin (Hyclone), and 100 $\mu\text{g}\cdot\text{mL}^{-1}$ streptomycin (Hyclone). The cells were maintained at 37 $^{\circ}\text{C}$ in a humidified incubator with 5% $\text{CO}_2/95\%$ air (*V/V*). Then the cells were stimulated with 0.5 $\mu\text{g}\cdot\text{mL}^{-1}$ of LPS in the presence or absence of the tested compounds and incubated for 24 h at 37 $^{\circ}\text{C}$.

Cell viability assay. The cytotoxicity of the isolated compounds was assessed using an MTT assay to determine the viability of RAW264.7 cells. Approximately 3×10^4 cells/mL (100 μL per well) were seeded in 96 well plates (Excell Bio) and incubated overnight. The cells were then treated with the tested compounds for 24 h. Cell viability was measured using the MTT assay, as previously described [22].

Bioassay for NO production. The concentration of nitrite in the medium, an indicator of NO production, was determined using the Griess method (Beyotime Biotechnology Co., Ltd.). The cell-free supernatant was mixed with an equal volume of 50 μL Griess reagent, and the absorbance of the resultant product was measured at 540 nm using a microplate reader. The nitrite concentration and inhibitory rate were calculated based on a standard calibration curve. The inhibitory effect of the tested compounds on LPS-induced NO production was described as IC_{50} values. Hydrocortisone (Shanghai Yuanye Bio-Technology Co., Ltd.) was used as a positive control.

Enzyme-linked immunosorbent assay (ELISA). Inflammatory cytokines were detected using an ELISA following a similar protocol to that used for NO detection. After treatment, cell supernatants were collected, and the production of IL-6 was measured using ELISA kits (4A Biotech Co., Ltd.) according to the manufacturer's instructions. Each assay was

performed in triplicate, and results were expressed as mean \pm standard deviation (SD).

Statistical analysis. Quantitative data are presented as mean \pm SD. Statistical analysis was performed using GraphPad Prism 4.0 software (GraphPad Software Inc). Differences between groups were assessed using one-way analysis of variance (ANOVA), followed by Tukey's post hoc test. A *P*-value of < 0.05 was considered statistically significant.

Supporting Information

HR-ESI-MS and 1D and 2D NMR spectra of compounds **1**, **2**, **8** and **12** can be requested by sending E-mails to the corresponding authors.

References

- [1] *Pharmacopoeia of the People's Republic of China (Part 1)* [S]. Beijing: China Medical Science Press; 2020.
- [2] Dar MY, Shah WA, Rather MA, et al. Chemical composition, *in vitro* cytotoxic and antioxidant activities of the essential oil and major constituents of *Cymbopogon jawarancusa* (Kashmir) [J]. *Food Chem*, 2011, **129**(4): 1606-1611.
- [3] Thapa P, Lee YJ, Nguyen TT, et al. Eudesmane and eremophilane sesquiterpenes from the fruits of *Alpinia oxyphylla* with protective effects against oxidative stress in adipose-derived mesenchymal stem cells [J]. *Molecules*, 2021, **26**(6): 1762.
- [4] Bian QY, Wang SY, Xu LJ, et al. Two new antioxidant diarylheptanoids from the fruits of *Alpinia oxyphylla* [J]. *J Asian Nat Prod Res*, 2013, **15**(10): 1094-1099.
- [5] He B, Xu F, Yan T, et al. Tectochrysin from *Alpinia Oxyphylla* Miq. alleviates $\text{A}\beta(1-42)$ induced learning and memory impairments in mice [J]. *Eur J Pharmacol*, 2019, **842**: 365-372.
- [6] Ji ZH, Zhao H, Liu C, et al. *In-vitro* neuroprotective effect and mechanism of 2 β -hydroxy- δ -cadinol against amyloid β -induced neuronal apoptosis [J]. *Neuroreport*, 2020, **31**(3): 245-250.
- [7] Han Y, Wu J, Liu Y, et al. Therapeutic effect and mechanism of polysaccharide from *Alpiniae oxyphyllae* fructus on urinary incontinence [J]. *Int J Biol Macromol*, 2019, **128**: 804-813.
- [8] Su MS, Xu L, Gu SG, et al. Therapeutic effects and modulatory mechanism of *Alpiniae oxyphyllae* fructus in chronic intermittent hypoxia induced enuresis in rats [J]. *Sleep Breath*, 2020, **24**(1): 329-337.
- [9] Zhang T, Qiu J, Wu X, et al. Schizonepeta tenuifolia with *Alpinia Oxyphylla* alleviates atopic dermatitis and improves the gut microbiome in Nc/Nga mice [J]. *Pharmaceutics*, 2020, **12**(8): 722.
- [10] Fang L, Yan Y, Xu Z, et al. Tectochrysin ameliorates murine allergic airway inflammation by suppressing Th2 response and oxidative stress [J]. *Eur J Pharmacol*, 2021, **902**: 174100.
- [11] Yoo E, Lee J, Lertpatipanpong P, et al. Anti-proliferative activity of *A. Oxyphylla* and its bioactive constituent nootkatone in colorectal cancer cells [J]. *BMC Cancer*, 2020, **20**(1): 881.
- [12] Dong J, Zhou M, Qin Q, et al. Structurally diverse new eudesmane sesquiterpenoids with anti-inflammatory activity from the fruits of *Alpinia oxyphylla* [J]. *Bioorg Chem*, 2023, **134**: 106431.
- [13] Liu T, Wu H, Jiang H, et al. Echingridimer A, an oxaspiro dimeric sesquiterpenoid with a 6/6/5/6/6 fused ring system from

- Echinops grijsii* and aphicidal activity evaluation [J]. *J Org Chem*, 2019, **84**(17): 10757-10763.
- [14] Staerk D, Skole B, Jørgensen FS, *et al.* Isolation of a library of aromadendranes from *Landolphia dulcis* and its characterization using the VolSurf approach [J]. *J Nat Prod*, 2004, **67**(5): 799-805.
- [15] Macias FA, Simonet AM, Pacheco PC, *et al.* Natural and synthetic podolactones with potential use as natural herbicide models [J]. *J Agric Food Chem*, 2000, **48**(7): 3003-3007.
- [16] Xin M, Guo S, Zhang W, *et al.* Chemical constituents of supercritical extracts from *Alpinia officinarum* and the feeding deterrent activity against *tribolium castaneum* [J]. *Molecules*, 2017, **22**(4): 647.
- [17] Honmore VS, Kandhare AD, Kadam PP, *et al.* Diarylheptanoid, a constituent isolated from methanol extract of *Alpinia officinarum* attenuates TNF- α level in Freund's complete adjuvant-induced arthritis in rats [J]. *J Ethnopharmacol*, 2019, **229**: 233-245.
- [18] Sun DJ, Zhu LJ, Zhao YQ, *et al.* Diarylheptanoid: a privileged structure in drug discovery [J]. *Fitoterapia*, 2020, **142**: 104490.
- [19] Kuo YH, Shiu LL. Two new sesquiterpenes, 12-hydroxy- α -longipinene and 15-hydroxyacora-4(14),8-diene, from the heartwood of *Juniperus chinensis* LINN. var. *tsukusiensis* MASAM [J]. *Chem Pharm Bull*, 1996, **44**: 1758-1760.
- [20] Hikino H, Suzuki N, Takemoto T. Sesquiterpenoids. XIV. aynthesis of cyperolone and 3-*epi*-cyperolone [J]. *Chem Pharm Bull*, 1967, **15**(9): 1395-1404.
- [21] Weng Y, Yu X, Li J, *et al.* Abietane diterpenoids from *Lycopodium complanatum* [J]. *Fitoterapia*, 2018, **128**: 135-141.
- [22] Qin DP, Li HB, Pang QQ, *et al.* Structurally diverse sesquiterpenoids from the aerial parts of *Artemisia annua* (Qinghao) and their striking systemically anti-inflammatory activities [J]. *Bioorg Chem*, 2020, **103**: 104221.

Cite this article as: DONG Jie, LI Haibo, ZHOU Mi, *et al.* Four new diarylheptanoids and two new terpenoids from the fruits of *Alpinia oxyphylla* and their anti-inflammatory activities [J]. *Chin J Nat Med*, 2024, **22**(10): 929-936.